Mon. Not. R. Astron. Soc. **000**, 1–6 (2002) Printed 21 October 2005 (MN LATEX style file v2.2)

A Laboratory Plasma Experiment for Studying Magnetic Dynamics of Accretion Discs and Jets

S. C. Hsu and P. M. Bellan
Dept. of Applied Physics, California Institute of Technology, Pasadena, CA 91125

ABSTRACT
This work describes a laboratory plasma experiment and initial results which should give insight into the magnetic dynamics of accretion discs and jets. A high-speed multiple-frame CCD camera reveals images of the formation and helical instability of a collimated plasma, similar to MHD models of disc jets, and also plasma detachment associated with spheromak formation, which may have relevance to disc winds and flares. The plasmas are produced by a planar magnetized coaxial gun. The resulting magnetic topology is dependent on the details of magnetic helicity injection, namely the force-free state eigenvalue $\alpha_{\rm gun}$ imposed by the coaxial gun.

Key words: accretion discs, MHD, plasmas, methods: laboratory

1 INTRODUCTION

The accretion disc occupies a leading role in astrophysics, figuring prominently in young stellar objects (YSO), binary star systems, and active galactic nuclei (AGN). An unsolved mystery is the origin of highly collimated bipolar jets and episodic flares associated with accretion discs. It was proposed some time ago that magnetic field dynamics can supply the necessary jet formation and collimation mechanisms (Blandford 1976; Lovelace 1976). Magnetohydrodynamic (MHD) simulations have shown that jets are a natural consequence of a rotating disc in the presence of a magnetic field (*e.g.* Shibata & Uchida 1985). Jet structure, such as "knots," and also episodic behavior are observed in the simulations (Ouyed & Pudritz 1997; Goodson, Böhm & Winglee 1999; Nakamura, Uchida & Hirose 2001). The details of these models are unlikely to be tested by observations anytime in the near future. Therefore, data from laboratory experiments could be very useful for this purpose. It should be noted that astrophysical jets have been compared theoretically with plasma guns (Contopoulos 1995), and that plasma experimentalists have interpreted coaxial gun plasma flows in the context of astrophysical jet morphology (Caress 1996).

This work describes a new plasma gun based laboratory experiment and initial results which should give insight into the magnetic dynamics of accretion discs and jets. This experiment is the first to use a plasma gun which explicitly simulates the geometry and topology of a magnetically-linked star-disc system by using a co-planar disc-annulus electrode setup. The experiment reveals (1) the formation and helical structure of a magnetically-driven collimated plasma, similar to proposed models of astrophysical jets, and (2) plasma detachment which may be relevant for disc winds and flares and field-line opening in disc coronae. The resulting magnetic topology depends on the details of magnetic helicity injection, namely the force-free state eigenvalue α imposed at the boundary. The plasmas in this work satisfy the MHD criteria globally ($S \gg 1$, $\rho_{\rm i} << L$, and $V_{\rm A} << c$, where S is the Lundquist number, $\rho_{\rm i}$ the ion gyro-radius, L the plasma scale length, and $V_{\rm A}$ the Alfvén speed). It should be noted that $S \sim 10^3$ in the experiment, similar to that in MHD numerical simulations.

This paper is organized as follows. Section II gives a qualitative description of how the magnetic dynamics of an accretion disc system are modeled in the laboratory. Section III describes the experimental setup. Section IV presents initial experimental results, and Sec. V provides a discussion. Finally, a summary is given in Sec. VI.

2 MODELING DISC MAGNETIC DYNAMICS IN THE LABORATORY

For non-relativistic accretion disc dynamics, such as in YSO's and some binary star systems, global magnetic field evolution can be described using MHD. The ideal MHD Ohm's law,

$$\mathbf{E} + \mathbf{U} \times \mathbf{B} = 0 \qquad (1)$$

implies that an electric field $\mathbf{E}$ will be induced due to the sheared toroidal rotation of the disc in the presence of a magnetic field $\mathbf{B}$. The $E_{\rm R}$ component creates an electric potential drop V between the central object and the accreting disc, and therefore magnetic helicity K will be injected into the disc magnetosphere at the rate $\mathrm{d}K/\mathrm{d}t = 2\psi V$ (*e.g.* Bellan 2000), where ψ is the poloidal magnetic flux emanating from the central object.

In the laboratory, a planar coaxial disc-annulus electrode setup simulates the topology and approximate geometry of the astrophysical star-disc system. However, rather than rotating the annulus to induce an $E_{\rm R}$ as in a real accretion disc, an electric potential $V_{\rm gun}$ is applied across the electrodes instead. The background poloidal $\mathbf{B}$, which corresponds to the field of the central object, is generated with an external coil. Again through Eq. (1), the background $\mathbf{B}$ and the applied voltage induce an $\mathbf{E}\times\mathbf{B}$ toroidal rotation in the plasma, achieving a magnetic helicity injection rate $\mathrm{d}K/\mathrm{d}t = 2\psi_{\rm gun}V_{\rm gun}$, where $\psi_{\rm gun}$ is the poloidal flux intercepting the inner disc electrode. This setup is commonly used to create spheromak plasmas (Rosenbluth & Bussac 1979; Jarboe 1994; Bellan 2000).

Therefore, the most basic magnetic dynamics near a star-disc system, namely the winding up of poloidal field lines generated by the central object by disc rotation, can be simulated in the laboratory by applying a voltage across coaxial electrodes in the presence of a background poloidal field. Of course there are limitations to the laboratory setup. For example, Keplerian sheared rotation and the existence and placement of a star-disc co-rotation radius cannot be exactly replicated. An experiment cannot hope to capture all the nuances and range of behaviors in all accretion disc systems. However, it can provide experimental data on the most fundamental plasma configurations which can result from a simple magnetically driven system.

3 EXPERIMENTAL SETUP

Figure 1 shows a side-view schematic of the experimental setup. A planar coaxial gun is installed on one end of a large vacuum chamber evacuated to 1.5×10^{-7} Torr. The chamber is large compared to the plasma so as not to affect the plasma evolution. The gun setup, enlarged in Fig. 2, includes (1) an inner electrode consisting of a 20.3 cm diameter copper disc (attached to end of blue re-entrant port), (2) an outer electrode consisting of a 50.8 cm outer diameter copper annulus (in green), (3) an external solenoid (in red) to produce a poloidal bias magnetic flux ψ linking the inner and outer electrodes, and (4) gas lines to deliver fast puffs of neutral hydrogen gas to the desired position of breakdown (adjacent to the electrodes). The gap between disc and annulus is 0.635 cm; plasma breakdown does not occur in the gap because the pressure-distance product there is too small to satisfy the Paschen breakdown criteria (Bellan 2000). A cylindrical coordinate system (R, θ, Z) is utilized, with the origin at the center of the inner electrode and $+Z$ defined to be away from the electrode (toward the left in Fig. 2). There are eight gas injection holes on each electrode, distributed uniformly along the θ direction of the inner and outer electrodes. The bias field is characterized by the parameter $\psi_{\rm gun}$, which is the total initial bias flux intercepted by the inner electrode; sample contours of ψ are shown in Fig. 2.

The plasma formation sequence is as follows. After the bias field and gas puffs are introduced, negative polarity high-voltage is applied to the inner electrode by discharging a 120 μF capacitor bank through an ignitron; the outer electrode is maintained at vacuum chamber ground. In the presence of the high-voltage, the neutral hydrogen breaks

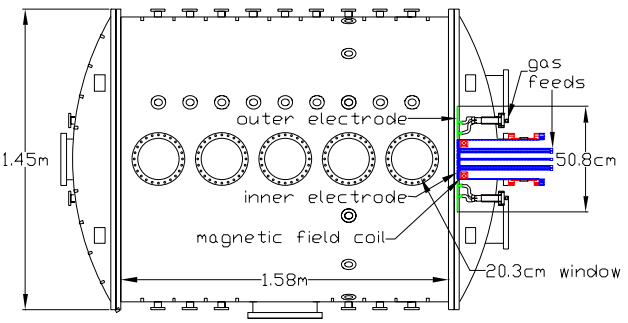

Figure 1. Side-view schematic of vacuum chamber and planar coaxial gun setup.

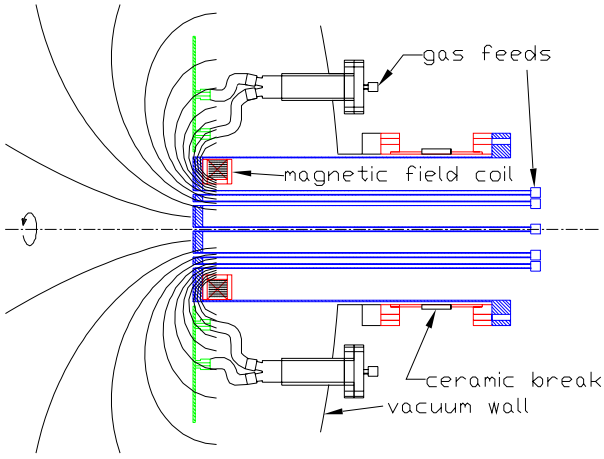

Figure 2. Side-view schematic of planar coaxial gun, including gas feeds, external magnetic field coil, poloidal flux ψ contours, and symmetry axis.

down. The optimum path for breakdown is along vacuum field lines linking the inner and outer electrodes as shown in Fig. 2. The gun voltage $V_{\rm gun}$ drives a current $I_{\rm gun}$ between the electrodes, twisting up the purely poloidal vacuum field and producing a B_θ. In an accretion disc, it is the disc rotation which achieves the same effect. The initally discrete flux tubes expand and eventually merge into an axisymmetric configuration. Throughout this process, magnetic helicity is being injected from the gun into the plasma.

Experimental results to date have centered around time-resolved global imaging of the plasma evolution. Images shown here were taken using a Cooke Corp. HSFC-PRO multiple-frame charge-coupled device (CCD) camera, which takes up to eight images per plasma discharge. The camera view is through the 20.3 cm window (labeled in Fig. 1) such that the gun electrodes appear on the right hand side of each frame. A false-color table is applied to the images for ease of viewing. Typically, the plasma is observed in unfiltered visible light. However, by using filters, it has been verified that most of the light emission is from neutral hydrogen line transitions. The exposure time of each frame is 20 ns and the interframe time is set typically to 1.5 μs, which is on the order of an Alfvén transit time. Additionally, a triple Langmuir probe is utilized to measure localized values of $n_{\rm e}$, $T_{\rm e}$, and floating potential. A Rogowski coil encircling the ceramic

break (see Fig. 2) measures $I_{\rm gun}$, and a high-voltage probe measures $V_{\rm gun}$ at the mouth of the re-entrant port (shown in blue in Fig. 2). Typical experimental parameters are as follows: $V_{\rm gun} \approx 4$–6 kV, $I_{\rm gun} \approx 70$–130 kA, $\psi_{\rm gun} \approx 0.5$–$2$ mWb, $B \sim 0.2$–1 kG, $T_{\rm e} \sim T_{\rm i} \approx 5$–$20$ eV, $n_{\rm e} \sim 10^{14}$ cm^{-3}, and global $\beta \equiv 2\mu_0 nk(T_{\rm e}+T_{\rm i})/B^2 \sim 0.02$–$0.1$.

4 INITIAL EXPERIMENTAL RESULTS

Because the plasma is relatively low-β, it is reasonable as a first approximation to consider it as nearly force-free with plasma currents nearly parallel to the magnetic field, *i.e.*

$$\nabla \times \mathbf{B} \simeq \alpha \mathbf{B}. \qquad (2)$$

Equation (2) implies that α is constant along field lines but not necessarily across them. Integrating Eq. (2) over the gun surface, it can be shown that the force-free state eigenvalue imposed by the gun is $\alpha_{\rm gun} = \mu_0 I_{\rm gun}/\psi_{\rm gun}$. Experimentally, both $I_{\rm gun}$ and $\psi_{\rm gun}$ can be adjusted to achieve a range of $\alpha_{\rm gun}$ values. Depending on the peak value of $\alpha_{\rm gun}$, several distinct plasma configurations are identified.

4.1 Collimated plasma: an analog for disc jets

For low values of $\alpha_{\rm gun}$, the formation of a collimated plasma is observed, as shown in Fig. 3. In this plasma, $\alpha_{\rm gun}$ peaks at approximately 66 m^{-1}. In Fig. 3(a), gas breakdown has just occurred along eight discrete paths, each of which follows vacuum magnetic field lines and terminates at gas injection holes. In frame (b), the discrete arcs have expanded and begun coalescing. Magnetic reconnection is expected to occur along the Z-axis as the discrete flux tubes coalesce; the particularly intense light emission there may be due to higher plasma density resulting from compression. In frames (c)–(d), a central column forms and expands in the Z-direction. In frames (e)–(g), the central column extends in length and persists for several Alfvén transit times. In frame (h), the central column begins to break up.

The bright structures in the images are expected to correlate with magnetic topology and current flow; this was verified previously in a similar experiment using direct measurements of magnetic field (Yee & Bellan 2000). This correlation is consistent with (1) the light emission being predominantly from neutral hydrogen atoms excited by current-carrying electrons and (2) the fact that the plasma is low-β and expected to be in a nearly force-free state in which $\mathbf{J}$ is nearly parallel to $\mathbf{B}$. It should be noted also that H–H$^+$ charge-exchange time is estimated to be very fast ($\ll 1$ μs) in this experiment, and therefore light emission may be representative of plasma ion dynamics. Filamentary structures can be seen inside the column, suggesting complex field topologies within the globally collimated structure.

The cross section of the central column is clearly observable in Fig. 3. If there are no collimating forces, clearly the length of the column would not be as elongated as observed, nor would the cross section be so uniform along the Z-direction. This result verifies that the necessary magnetic structure and collimation for a disc jet can arise from magnetic forces associated with helicity injection.

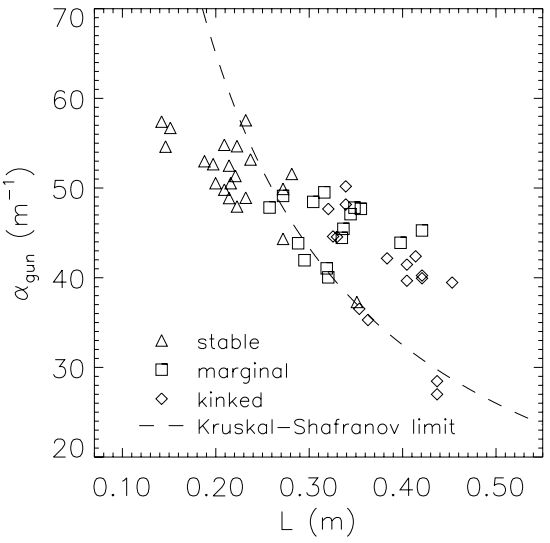

Figure 5. A plot of $\alpha_{\rm gun}$ versus column length L for different plasmas, showing good agreement with the Kruskal-Shafranov condition for a current-driven kink instability.

4.2 Helical instability: an analog for jet structure

Higher $\alpha_{\rm gun}$ results in plasmas with unstable central columns, as shown in Fig. 4, in which $\alpha_{\rm gun}$ peaks at approximately 71 m^{-1}. In Fig. 4(e), a highly nonlinear helical perturbation appears in the collimated plasma. By altering the CCD camera timing, it is possible to determine the characteristic growth time of the instability, which is about 1.7 μs, similar to the characteristic Alfvén time. The instability appears to be an ideal current-driven kink mode.

The Kruskal-Shafranov condition for ideal kink stability in a cylindrical column is (*e.g.* Bateman 1978)

$$q_{\rm edge} = 2\pi a B_{\rm Z}/LB_\theta > 1, \qquad (3)$$

where a is the column radius and L the column length. Assuming that both the initial $\psi_{\rm gun}$ and the instantaneous $I_{\rm gun}$ are fully contained inside the plasma column, and using the definition of $\alpha_{\rm gun}$ and $\psi_{\rm gun}$, it is straightforward to show that the condition for stability is

$$\alpha_{\rm gun} L < 4\pi. \qquad (4)$$

Figure 5 plots $\alpha_{\rm gun}$ versus L for a collection of central columns taken from both different discharges and different times from within the same discharge. Stable (triangles), marginally unstable (squares), and kinked (diamonds) columns are plotted in $\alpha_{\rm gun}$–L space, along with the Kruskal-Shafranov stability threshold (dashed line), showing good agreement between experiment and theory. This result indicates that plasma instabilities, in this case an ideal kink, can give rise to macroscopic structure within jets.

4.3 Detached plasma: an analog for disc flares

Still higher values of $\alpha_{\rm gun}$ result in detached plasmas, as shown in Fig. 6, in which $\alpha_{\rm gun}$ peaks at approximately 129 m^{-1}. In this discharge, the plasma appears to detach from the electrodes in frame (d) and then propagates along

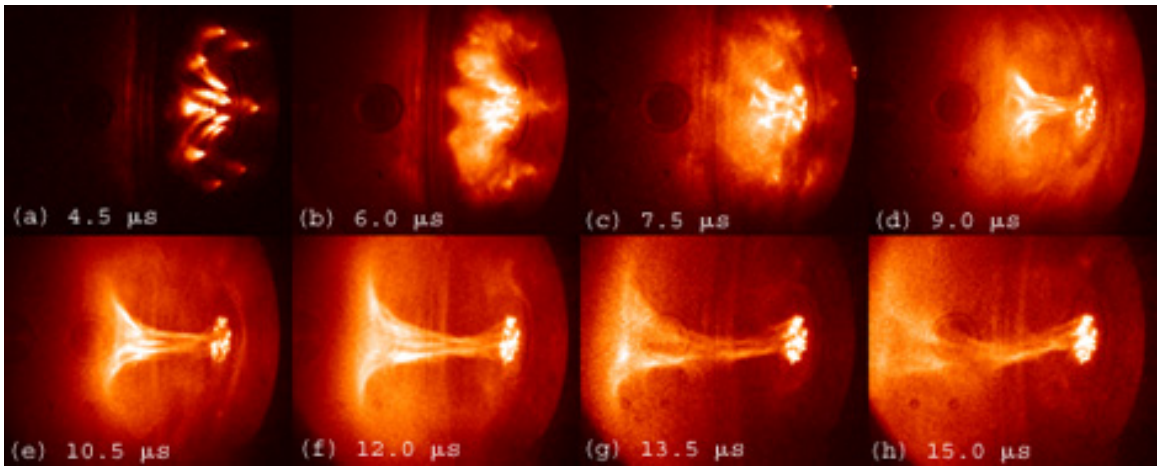

Figure 3. Images of plasma evolution (shot 1210; peak $\alpha_{\rm gun} \approx 66$ m^{-1}) in which a plasma column forms and persists for many Alfvén transit times, illustrating the magnetic topology required for an astrophysical jet.

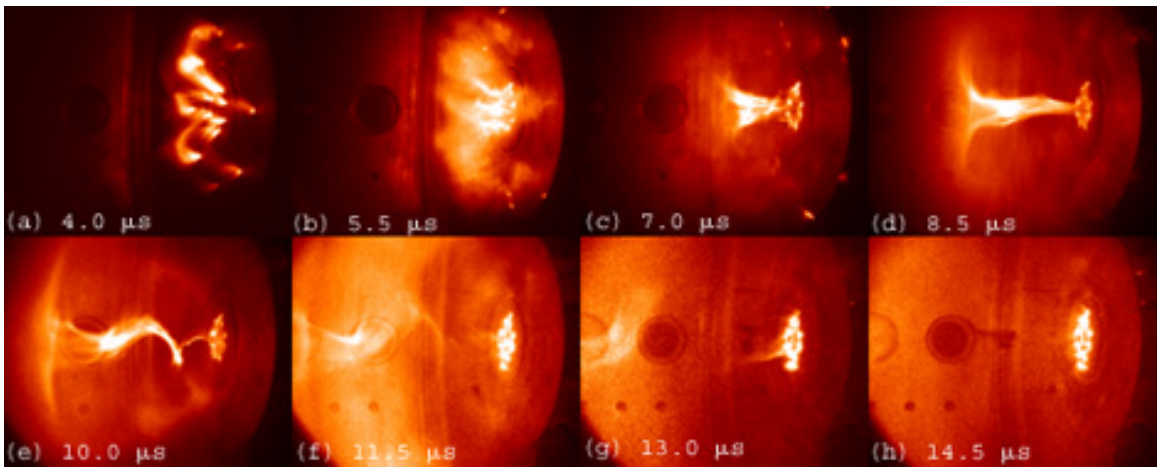

Figure 4. Images of plasma evolution (shot 1233; peak $\alpha_{\rm gun} \approx 71$ m^{-1}) in which a helical instability, likely a current-driven kink, develops on the ideal MHD timescale, illustrating one possible source of jet internal structure.

the Z direction at a speed of approximately 6×10^4 m/s, a fraction of the estimated $V_{\rm A}$. It is likely that a spheromak configuration is formed here; this was verified previously with direct measurement of **B** on an experiment with a non-planar source but similar helicity injection (Yee & Bellan 2000). This result supports the idea of field line reconnection above accretion discs, which can lead to disc winds and also episodic high energy flaring.

5 DISCUSSION

The results above show three distinct plasma configurations having accretion disc characteristics. All three configurations result from the same plasma formation process, the only difference being the peak value of the parameter $\alpha_{\rm gun} = \mu_0 I_{\rm gun}/\psi_{\rm gun}$. Figure 7 illustrates this dependence by placing different plasmas into $I_{\rm gun}$–$\psi_{\rm gun}$ parameter space, with detachment at larger $\alpha_{\rm gun}$, attached columns at lower $\alpha_{\rm gun}$, and kinked columns near $\alpha_{\rm crit} \approx 60$–$70$ m^{-1}.

This $\alpha_{\rm gun}$ dependence has many implications. Most importantly, it suggests that the plasma configurations associated with accretion discs and jets are related to Taylor relaxation theory (Taylor 1986), which is a description of how a plasma evolves as magnetic energy is minimized subject to the constraint of constant magnetic helicity. This process can be cast as a variational problem, and it can be shown that the resulting magnetic field configuration satisfies Eq. (2) with uniform α. In the case of a driven plasma like an astrophysical jet, $\nabla\alpha$ will be non-zero, and magnetic helicity will flow from regions of high to low α, which tends to "relax" the plasma toward uniform α (Bellan 2000). The evolution of many laboratory plasmas, including spheromaks, can be understood in terms of Taylor relaxation. For example, it has been shown that a threshold $\alpha_{\rm crit}$ at the source must be exceeded in order to form the closed-field configuration of a spheromak (*e.g.* Yee & Bellan 2000). This property is not surprising since analytic solutions of Eq. (2) show that **B** transitions from sinh-like to sine functions above a critical α (Bellan 2000).

Well-known models of astrophysical jets have considered separately the roles played by poloidal (Blandford & Payne 1982) and toroidal fields (Contopoulos 1995) in jet formation. However, the present work shows that jet struc-

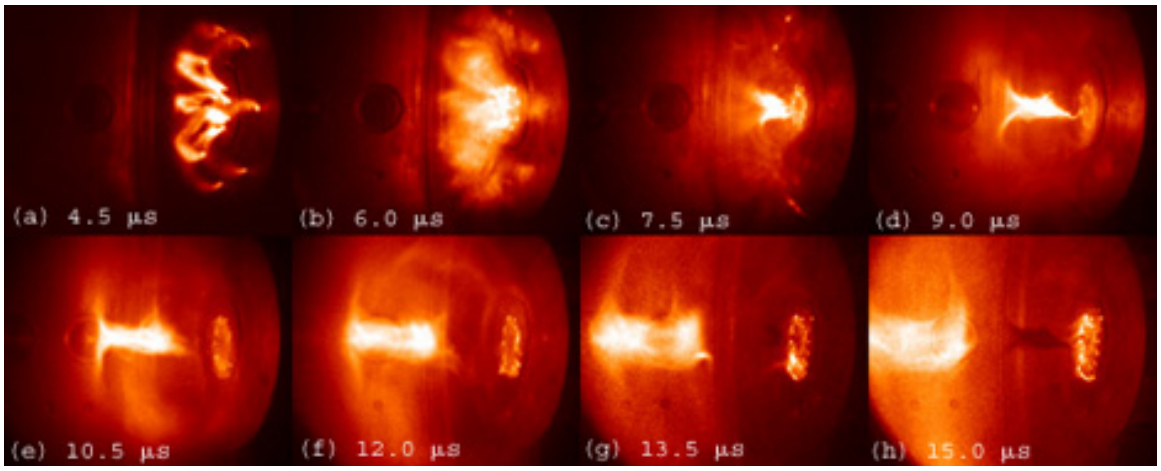

Figure 6. Images of plasma evolution (shot 1181; peak $\alpha_{\rm gun} \approx 129$ m^{-1}) in which the plasma detaches from the electrodes, illustrating the possibility of field-line opening in disc coronae.

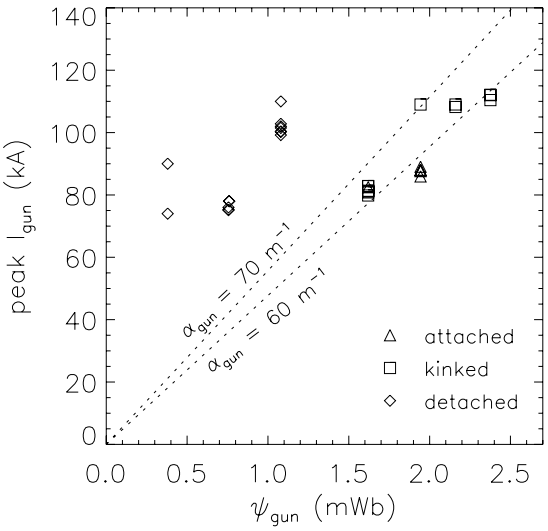

Figure 7. A plot of peak $I_{\rm gun}$ versus $\psi_{\rm gun}$ for a collection of plasma shots, showing the dependence of the plasma evolution on the peak value $\alpha_{\rm gun} = \mu_0 I_{\rm gun}/\psi_{\rm gun}$, with $\alpha_{\rm crit} \approx 60$–$70$ m^{-1}.

ture should result when the correct value of α occurs at the disc boundary, resulting in a non-arbitrary combination of poloidal and toroidal fields in the disc corona. Likewise, deformation of the jet structure will occur under different choice of α. In the experiment, the observed instability is consistent with an ideal current-driven kink. This instability has been observed in numerical simulations of AGN radio jets (Nakamura, Uchida & Hirose 2001) and proposed as the responsible mechanism for wiggled structure in the jets.

6 SUMMARY

A plasma gun based laboratory experiment approximates the boundary conditions and topology of a star-disc system, and it is shown experimentally that magnetic helicity injection with these boundary conditions leads naturally to both collimated plasmas and detached plasmas, suggestive of disc jets and flares, respectively. The onset of a helical instability in the plasma column is shown to be consistent with the Kruskal-Shafranov condition for an ideal current-driven kink. The magnetic topology depends on the force-free state eigenvalue $\alpha_{\rm gun}$ imposed at the plasma gun. It is argued that Taylor relaxation provides a useful description of the magnetic structures of accretion discs and jets. These results demonstrate experimentally that the concept of magnetically-driven jets is a viable one. More quantitative characterization of the observed plasmas is planned. This will include direct measurements of the magnetic field via insertable probes, ion flow velocity along the collimated plasma via Doppler spectroscopy, and plasma pressure profiles via Langmuir probes.

ACKNOWLEDGMENTS

The authors are grateful to J. Hansen, S. Pracko, C. Romero-Talamás, and F. Cosso for technical assistance. This work was supported by a U.S. Dept. of Energy (US-DoE) Fusion Energy Postdoctoral Fellowship and US-DoE contract no. DE-FG-03-98ER54461.

REFERENCES

Bateman G., 1978, MHD Instabilities, MIT Press, Cambridge
Blandford R. D., 1976, MNRAS, 176, 465
Blandford R. D., Payne D. G., 1982, MNRAS, 199, 883
Bellan P. M., 2000, Spheromaks, Imperial College Press, London
Caress R. W., 1996, MS thesis, North Carolina State University
Contopoulos J., 1995, ApJ, 450, 616
Goodson A. P., Böhm K.-H., Winglee R. M., 1999, ApJ, 524, 142
Jarboe T. R., 1994, Plasma Phys. Control. Fusion, 36, 945
Lovelace R. V. E., 1976, Nature, 262, 649
Nakamura, M., Uchida Y., Hirose S., 2001, New Astron., 6, 61
Ouyed R., Pudritz R. E., 1997, ApJ, 484, 794
Rosenbluth M. N., Bussac M. N., 1979, Nucl. Fusion, 19, 489
Shibata K., Uchida Y., 1985, PASJ, 37, 31
Taylor J. B., 1986, Rev. Mod. Phys., 58, 741
Yee J., Bellan P. M., 2000, Phys. Plasmas, 7, 3625

This paper has been typeset from a TEX/ LATEX file prepared by the author.